Supporting Information

RESULTS

MCF-10A verification assays. To verify that these results are not specific to the lineage of the parental cell type in which the reporter is constructed, we also constructed a reporter in MCF-10A cells (1). MCF-10A cells are non-tumorigenic, human mammary epithelial cells which are distinct in lineage from NIH 3T3 which are immortalized mouse mesenchymal cells. Additionally, MCF-10As are a commonly used cell line and are well characterized (2). Voltage (Figure S4A) and frequency (Figure S4B) sweeps performed with the MCF-10A cell line were comparable to those obtained with the NIH-3T3 cell lines, the main difference being that the time dynamics of the expression of these cells was different.

SUPPORTING MATERIALS & METHODS

Cell culture. MCF-10A cells were obtained from the ATCC. MCF-10A cells were cultured in defined mammary epithelial growth media (CC-2571, MEGM Bullet Kit, Lonza, Inc.) supplanted with bovine pituitary extract and epidermal growth factor. MCF-10A cells were dissociated using Accumax (Innovative Cell Technologies) for 15 minutes at 37 °C and then quenched with specially prepared quenching media (DMEM with 20% fetal bovine serum). Accumax was used in lieu of trypsin EDTA as it was more effective in dissociating clumped cells and in generating more uniform single cell suspensions when performing seeding. Cells were then spun down at 1000 rpm for 5 minutes. The supernatant was subsequently aspirated and supplanted with MEGM-based media. The cell pellet was then broken up by gentle trituration. The cells were then split at 1:2 split ratio to continue routine culture.

RNA interference. Lentiviral pLKO.1-puro short-hairpin RNA (shRNA) constructs were provided courtesy of Chengkai Dai. RNA interference using these lentiviral vectors has been previously described (3). Briefly, genes encoding *H-RasV12D, PDGF-B*, myristoylated *AKT1*, *v-SRC*, *MYC*, and *LTA* were cloned into the retroviral vector pBABE-zeo. Stable virus packaging cell lines were prepared by transfecting individual plasmids into EcoPack2-293 cells using Lipofectamine (Invitrogen) followed by zeocin selection. Lentiviruses were then produced by transiently co-transfecting individual shRNA constructs together with plasmids encoding ΔVPR and VSV-G together into 293T cells using Fugene 6 (Roche Diagnostics GmbH). Viral supernatants were collected and filtered through 0.45μm syringe filters. Viral transduction was achieved by incubating target cells with viral supernatants containing 5 μg/L polybrene overnight. The *HSF1*-targeted sequences are as follows: C2: 5'-GCTGCATACCTGCTGCCTTTA-3'; C3: 5'-CCCTGAAGAGTGAGGACATAA-3'; hA6: 5'-GCAGGTTGTTCATAGTCAGAA-3'; hA8: 5'- CCAGCAACAGAAAGTCGTCAA-3'; and hA9: 5' GCCCAAGTACTTCAAGCACAA-3'. Total protein content of cells was verified using Western blotting protocols.

Western blotting. Whole-cell protein extracts were prepared in cold lysis buffer consisting of: 100 mM NaCl, 30 mM Tris-HCl (pH 7.6), 1% NP-40, 30 mM sodium fluoride, 1 mM EDTA, 1 mM sodium vanadate, and complete protease inhibitor cocktail tablet (Roche Diagnostics). Samples were incubated on ice for 30 min and supernatants were recovered by centrifugation at 14,000 rpm at 4°C for 10 min. Protein concentrations were determined using BCA colorimetric reagent (Pierce Biochemical) and spectrophotometric absorption at 562 nm. Proteins were then separated on NuPAGE Novex gels (Invitrogen) and transferred to PROTRAN nitrocellulose membrane (Whatman). After transfer, membranes were stained with Ponceau (Pierce Biochemical) to assess equal loading and imaged using white light illumination on a gel documentation system. Stock wash solutions (5× TBSS) were prepared using 100 mM Tris (v/v) pH 7.6, 0.25% (v/v) Tween 20 and 4.5% (w/v) NaCl. After imaging, the membrane was de-stained by rinsing briefly in water and then 2-3× in 1× TTBS for about 5 min (ensuring the red stain is no longer visible). Blocking buffer (BB) was prepared using 3% (w/v) nonfat Carnation milk powder in 1× TTBS (pH should be readjusted with NaOH to pH 7.6 if necessary). Membranes were then blocked in BB for 1 hour and subsequently washed with PBS (pH 7.4) containing 0.1% Tween-20. Membranes were probed with the following antibodies - HSF1 (4356, ThermoFischer Scientific) diluted 1:50 (v/v) in BB and β-Actin (RB9421, ThermoFischer Scientific) diluted 1:100 (v/v) for 1hr at room temperature. Blotted membranes were subsequently washed in 5× (for 5 min each) with 1× TTBS. The secondary antibody was diluted to 1:20,000 (v/v) in BB and incubated for 1 hour at room temperature with the blotted membrane. The membrane was subsequently washed in 5× (for 5 min each) with 1× TTBS. To perform the detection, reagents for enhanced chemiluminescence were mixed 1:1 and incubated with the blot for 5 min on a plate rocker (ensuring that reagents were gently washing over the blot and keeping it moist). The blot was then carefully removed using tweezers, left to dry in air briefly (1-2 min) and then covered with Saran Wrap and placed on photographic film for 1 min in a dark room. The film was subsequently developed in an automated development system, and digitally scanned using a flat-bed scanner.

Image cytometry. In the case of weakly reporting cells and control cell populations, the DsRed-image is imperative for correctly identifying the number of cells. This scenario is depicted in Figure S6 (the standard imaging technique is shown in Figure S5). Once the cells are correctly identified in the EGFP image, each cell is marked and its corresponding fluorescence intensity is determined by summing across the entire cell area and then normalizing across the cell area. The average fluorescence intensity per cell is then averaged for the entire electrode and normalized to the average fluorescence intensity from the negative control electrode. The mean and standard deviation are plotted as a data point on each plot (hence each data point on the plot originates from ~100 single cells). It should be emphasized that both the image acquisition and analysis techniques presented here are highly automated with minimal user intervention, with the exception of the set up of the image acquisition, the rest of the steps can be completely

automated enabling the ability to perform more complex, high-content screens with the same platform and algorithms (and possibly a different reporter cell line).

Autofocus routines. The autofocus algorithm implemented in MATLAB, takes images at different focal planes and stores the intensity profile across the evenly spaced line features. This intensity profile is compared to a previously stored, best-plane-of-focus profile taken prior to the start of the experiment (only one of these profiles is stored, as the autofocus features are the same for each electrode). The difference between the profiles at each plane and the best-plane-of-focus profile is then stored and compared to each other. By choosing the plane of focus that has the least spatial variation in differential intensity, the best plane of focus is determined. The microscope *z*-stage position value stored for that particular focal plane is then chosen as the plane-of-focus for that experiment.

Resistor calibration. On-chip resistors are calibrated by using an adhesive-backed thermocouple (SA1-T, Omega) and placing it on the resistor. The chip is then placed on a hot plate and the temperature is ramped in ~ 5 °C increments starting at room temperature. The resistance value of the resistor is tabulated using a mulitmeter. The characteristic curve for the resistor is plotted and fitted to a straight line. This fitted function is then used to determine temperature from resistance. This procedure is repeated for each resistor on-chip as resistance values can vary across the device due to non-uniformities in the fabrication process.

Microfabrication. Devices were fabricated starting with double-width (50 x 75 mm), indium tin oxide (ITO) coated glass slides with resistivity of 5-8 Ω/ (SPI Supplies, Inc.). The ITO-coated glass slides were first cleaned with alternating 3× acetone and isopropanol rinses followed by a thorough rinse in DI water. Slides were subsequently baked at 150 °C for 30 minutes to remove any residual moisture. Slides were then coated with thin positive photoresist, OCG-825 (dynamic dispense, 750 rpm ramp, 5s, and final spin 1000 rpm for 35s) and the pre-baked at 90 °C for 30 minutes. Slides were then aligned and exposed on an i-Line ultraviolet exposure system (MA-4, Karl Suss). Exposed slides were subsequently developed in OCG 94 1:1 developer for 35 seconds. Developed slides were carefully observed under a fluorescence microscope to confirm that features had been accurately developed. The ITO features were then etched in dilute (1:1) hydrochloric acid for 20 minutes. The transparent nature of the film can make etch-termination processes difficult to visually characterize and to this end electrical measurements were made across the ITO features to ensure that no residual film remained. ITO-etched slides were 3× rinsed in DI water and subsequently dehydration-baked for 30 minutes at 150 °C. Slides were then coated with NR7-3000P lift-off resist to fabricate the temperature-sensing resistors, contact-pads and individual routing lines to each electrode patch. The slides were then coated in NR-7 negative tone lift-off resist (NR-7-3000P, Futurrex, Inc.) using static-dispense techniques, 750 rpm (5 second) spread, and 1500 rpm (35 second) spin. Slides were then soft-baked at 100 ºC on hot plates (with care being taken to read the actual plate

temperatures using a thermocouple) for 15 minutes. Slides were then exposed with i-Line ultra violet exposure (4 mJ/cm^2) for 25 seconds using a mask alignment tool (MA-4, Karl Suss). The slides were then post-baked at 150 ºC for 15 minutes (again, with careful attention to the actual plate temperature measurement). Slides were subsequently developed in custom developer solution (RD6, Futurrex, Inc.) and then triple-rinsed in DI water. Slides were then loaded in an electron beam deposition system for coating with 100 Å of titanium and 1000 Å of gold (using pre-determined recipes). Gold-coated slides were then placed in a resist remover solution (RR4, Futurrex, Inc.) overnight to lift-off the NR7 resist. Stringers and extraneous metal film were removed by rinsing in DI water. Top electrode slides were fabricated in an analogous fashion with the exception that the ITO etching step was not required as the feature sizes are extremely large.. Silicone membranes that serve as discrete wells for holding the cells and as spacers between the top and bottom electrodes are fabricated using laser-cutting techniques. Briefly, silicone sheets (125 μm thick, McMaster Carr Corporation) were clad between two transparency sheets and placed on the laser-cutter (Universal X2-660) bed and aligned to the cutting origin. Well patterns were drawn in software (CorelDraw 12) and after setting up the laser-cutter parameters (70% power, 50% speed and 1000 ppi), a dummy run is made to ensure that the membrane is correctly aligned. After cutting has completed, the membranes are cleaned with isoproponal and then autoclaved prior to use.

Waveform generation and signal-routing system. The waveform generation and signal routing system enables autonomous and efficient multiplexing of electric-field screening. The system consists of a custom-designed printed circuit board (PCB) with a bank of 16 voltage, controlled reed relays (PRMA1A05B, Digikey). A simple schematic of the system is depicted in Figure S1. Timing waveforms in transistor-transistor logic (TTL) format are generated using an off-the-shelf TTL generator (NI-6210, National Instruments). Additionally, connections from resistors were made to a universal serial bus (USB) controlled resistance/temperature logging unit (USB-Temp, Measurement Computing). This unit was used to log the resistance of each on-chip resistor over the course of the experiment (on-chip resistors were calibrated as described in the Supplementary Information section). The overall system was controlled through the generation of a waveform using a computer-controlled waveform generator (Agilent Technologies). A MATLAB script is used to generate the initial waveform for stimulation and subsequently set the TTL-generator's pulse to high and thereby route the waveform to the first electrode site. A computerized timer then counts down from the specified time for stimulation and subsequently commands the generation of the next the waveform and routes it to the next electrode site and repeats the process for all 16 electrode sites. The overall MATLAB script therefore describes the entire experiment from the amplitude and frequency of the waveform and the duration of its exposure to the cells.

Cell proliferation assays. Proliferation assays were performed at two voltage and frequency conditions. Numbers of cells were determined by automated microscopy (by identifying and

counting of cells using DsRed fluorescence signal). Cells were allowed to grow for 32 hours post-exposure and were imaged at three time points, before electric field exposure, 16 hours after exposure and 32 hours after exposure. Numbers of cells indicate that for the conditions studied, cells were able to grow after exposure and there was not a significant difference in numbers of cells from the initial population dying between seeding (blue bars in Fig. S11A,B) and exposure to the stimulus (green bars in Fig. S11A,B). Results for these assays are summarized in Figure S11 where each bar represents the average of experiments performed in triplicate (on a single chip) and error bars represent one standard deviation. Differences between the before (blue) and 32 hours after stimulus (red) conditions are statistically significant ($p<0.05$).

FIGURE LEGENDS

Fig. S1: Flow cytometry of reporter activation. Flow cytometric analysis of EGFP expression before (left) and after (right) stress induction showing a ~50× increase in expression post-stress.

Fig. S2: RNAi knockdown of Hsf1. Knockdown of Hsf1 abrogates the response of stress reporter cells indicating the stable integration of HSP70 promoter and correctly functioning heat shock pathway. (B) Western blotting showing that Hsf1 protein levels are indeed knocked down by construct C6 (red arrowhead) as compared to normal control (blue arrowhead). Actin protein levels remain the same across all samples.

Fig. S3: Quantitative imaging. Composite image (left) showing multiple scan points from a single electrode. Multi-wavelength fluorescence imaging of each region of the electrode allows using DsRed images to mask the GFP images and extract quantitative information from single cells in the GFP image (right). Scale bar 40 μm.

Fig. S4: Quantitative imaging (control populations). Constitutive DsRed expression plays an important role in the identification of weakly expressing fluorescent cells. The GFP image shows a near uniform fluorescence intensity with no evidence of cellular structures. The DsRed channel however, enables the visualization of these features. Masking these features then enables the identification of the cellular features. The algorithm then discriminates between both acellular features and clumps of cells ('Masked GFP' image). The resultant single cell fluorescence data is shown in the plot.

Fig. S5: Cell-based sensor repeatability across passage number. Red, green and blue traces indicate expression from passage 0 (defined arbitrarily), 1 and 2 cells respectively, with a maximum of 4.2% deviation in expression, which is statistically insignificant ($p<0.05$ via t-test).

Fig. S6: MCF-10A reporter results. A single-cell cloned reporter cell line generated in MCF-10A showed results comparable to those obtained with the NIH-3T3 reporter cell line. (A) Voltage sweep at 10 MHz shows an increasing trend of stress with increasing voltage and consequently increasing Joule heating. (B) Frequency sweep at 4 V_{pp} shows increased stress at low frequencies with lower stress levels at frequencies higher than 1 MHz. This trend mirrors that seen with the fibroblast cell line.

Fig. S7: Resistor calibration. Blue line shows characteristic fit (with $R^2 = 0.9819$) to measured temperature dependence (red circles) of on-chip resistors. Such fitted functions are used to determine temperature from resistance during temperature and voltage sweep experiments.

Fig. S8: Impedance measurements. Magnitude of impedance of a single well on the 16-well device loaded with culture media (oscillator voltage, 500 mV). Impedance is seen to be nearly constant (with 6.8% deviation) across two orders of magnitude in frequency.

Fig. S9: Electrical stimulation setup. A custom-designed computer-controlled relay box (dashed line) switches sinusoidal waveforms from a function generator to each individual electrode site. The entire electrical stimulation system resides outside of the incubator while the electrode array resides within the incubator at physiological conditions. Resistance measurements from each temperature sensitive-resistor at each electrode site are logged via a USB-controlled resistance logging unit. Steady-state temperatures are determined by fitting logged values to pre-determined calibration curves.

Figure S10: Fabrication processes. (A) Dual mask process for patterning electrode sites, temperature sensing resistors and routing. (B) Maskless process for fabricating silicone spacers to define volume for each electrode well.

Figure S11: Proliferation assays. Cell counts from two conditions of the voltage sweep at 2 Vp-p at 1 MHz and 6 Vp-p at 1 MHz (A) and two conditions of the frequency sweep at 4 Vp-p at 250 kHz and 9Vp-p at 10 MHz. Bars represent average cell counts after seeding and before exposure to electric-field stimulus (blue), 16 hours after exposure to stimulus (green) and 32 hours after exposure (red). Error bars represent one standard deviation.

Supporting Information References:

1. Soule HD, McGrath, C. M. (1986) A simplified method for passage and long-term growth of human mammary epithelial cells. *In Vitro* **22,** 6-12.
2. Soule HD, Maloney, T. M., Wolman, S. R., Peterson, W. D. Jr, Brenz, R., McGrath, C. M., Russo, J., Pauley, R. J., Jones, R. F., and Brooks, S. C. (1990) Isolation and characterization of a spontaneously immortalized human breast epithelial cell line, MCF-10. *Cancer Research* **50,** 6075-6086.
3. Dai C, Whitesell, L., Rogers, A. B., and Lindquist, S. (2007) Heat Shock Factor 1 is a powerful multifaceted modifier of carcinogenesis. *Cell* **130,** 1005-1018.

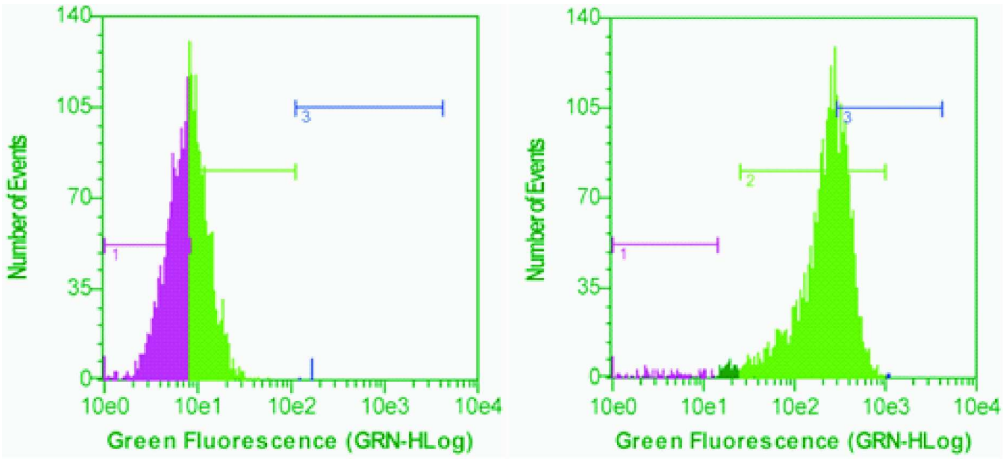

Fig. S1: Flow cytometry of reporter activation. Flow cytometric analysis of EGFP expression before (left) and after (right) stress induction showing a ~50× increase in expression post-stress.

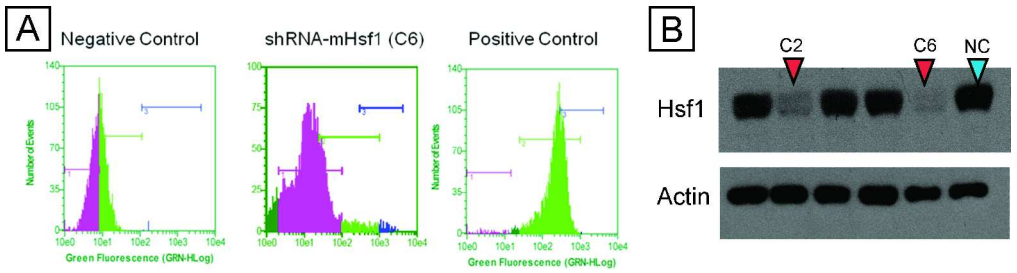

Fig. S2: RNAi knockdown of Hsf1. Knockdown of Hsf1 abrogates the response of stress reporter cells indicating the stable integration of HSP70 promoter and correctly functioning heat shock pathway. (B) Western blotting showing that Hsf1 protein levels are indeed knocked down by construct C6 (red arrowhead) as compared to normal control (blue arrowhead). Actin protein levels remain the same across all samples.

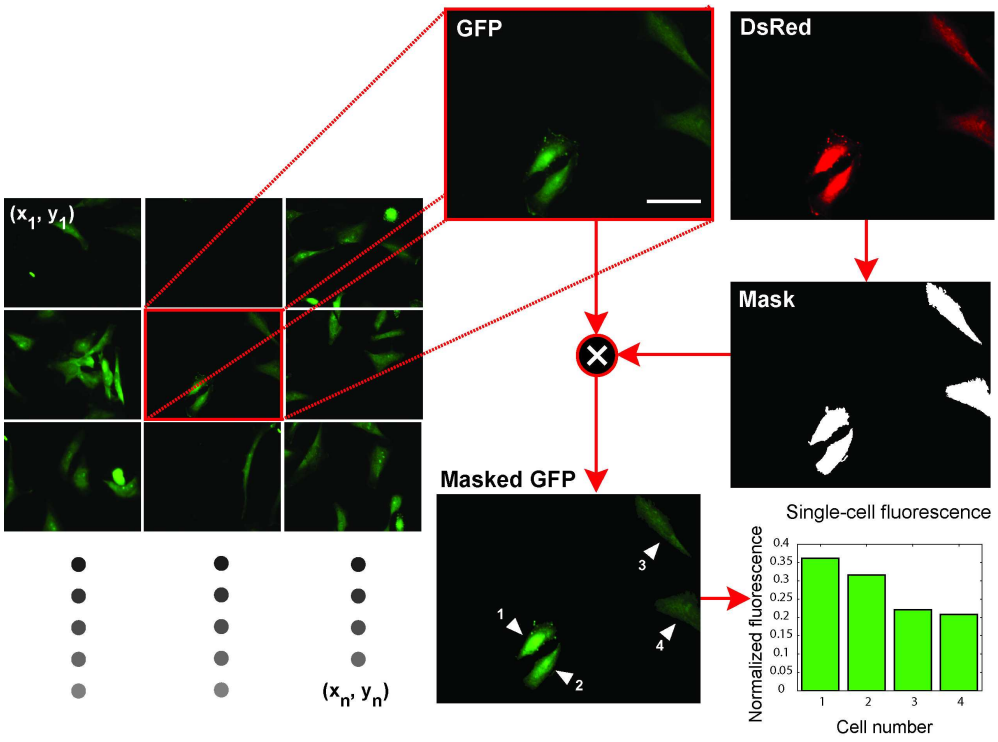

Fig. S3: Quantitative imaging. Composite image (left) showing multiple scan points from a single electrode. Multi-wavelength fluorescence imaging of each region of the electrode allows using DsRed images to mask the GFP images and extract quantitative information from single cells in the GFP image (right). Scale bar 40 μm.

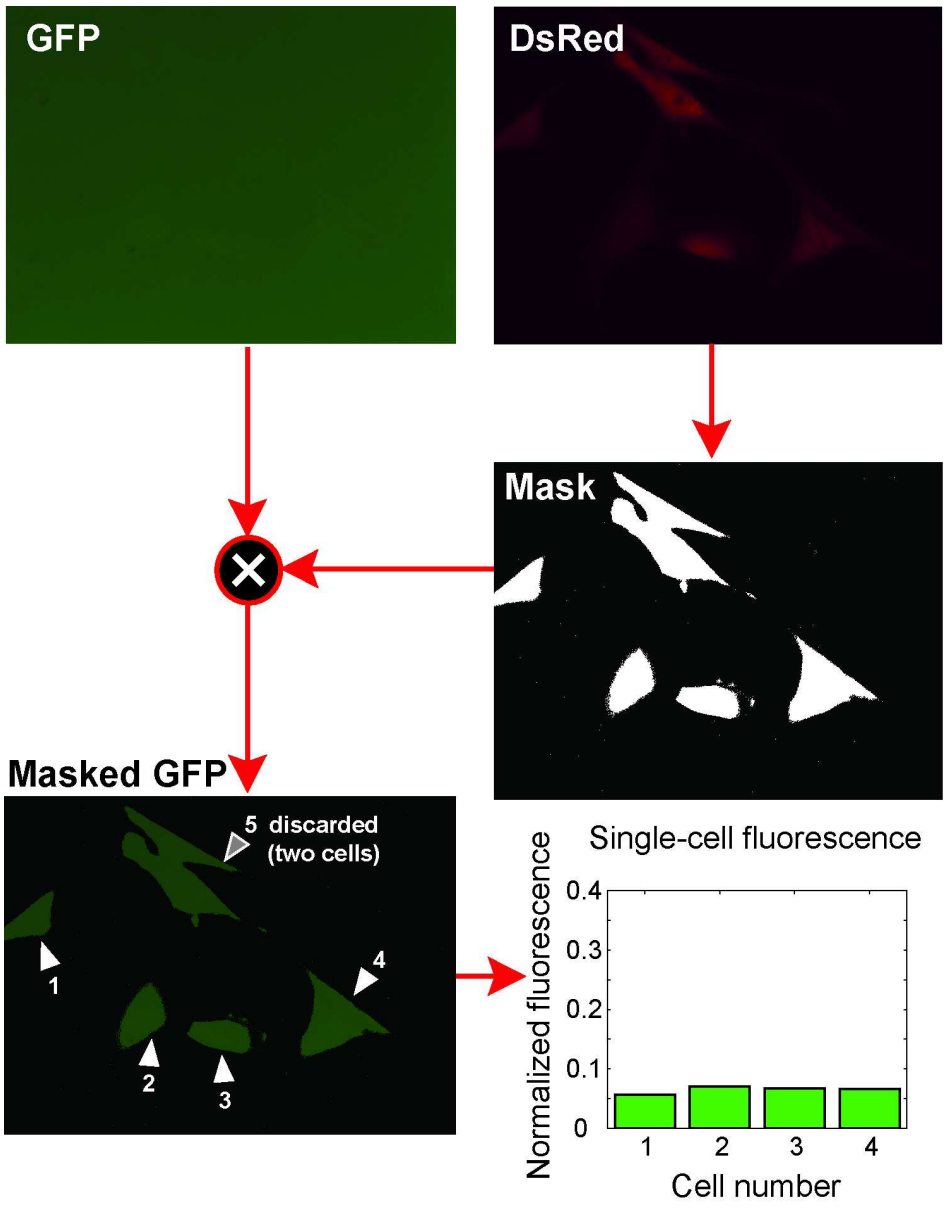

Fig. S4: Quantitative imaging (control populations). Constitutive DsRed expression plays an important role in the identification of weakly expressing fluorescent cells. The GFP image shows a near uniform fluorescence intensity with no evidence of cellular structures. The DsRed channel however, enables the visualization of these features. Masking these features then enables the identification of the cellular features. The algorithm then discriminates between both acellular features and clumps of cells ('Masked GFP' image). The resultant single cell fluorescence data is shown in the plot.

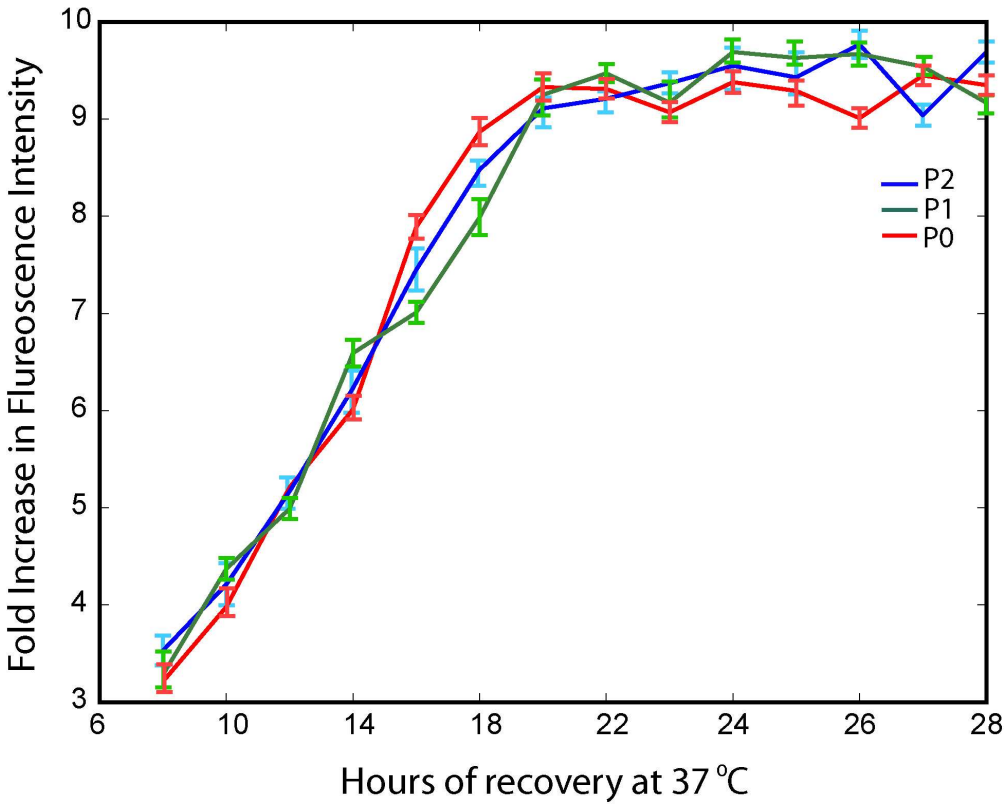

Fig. S5: Cell-based sensor repeatability across passage number. Red, green and blue traces indicate expression from passage 0 (defined arbitrarily), 1 and 2 cells respectively, with a maximum of 4.2% deviation in expression, which is statistically insignificant ($p<0.05$ via t-test).

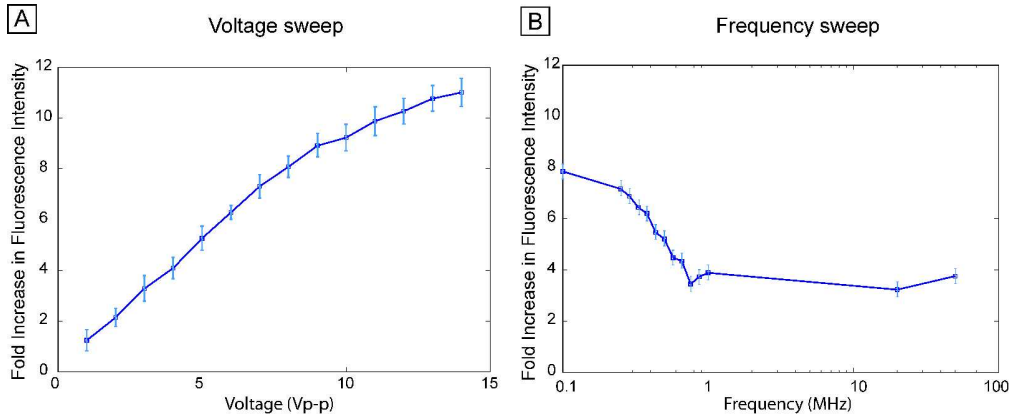

Fig. S6: MCF-10A reporter results. A single-cell cloned reporter cell line generated in MCF-10A showed results comparable to those obtained with the NIH-3T3 reporter cell line. (A) Voltage sweep at 10 MHz shows an increasing trend of stress with increasing voltage and consequently increasing Joule heating. (B) Frequency sweep at 4 Vpp shows increased stress at low frequencies with lower stress levels at frequencies higher than 1 MHz. This trend mirrors that seen with the fibroblast cell line.

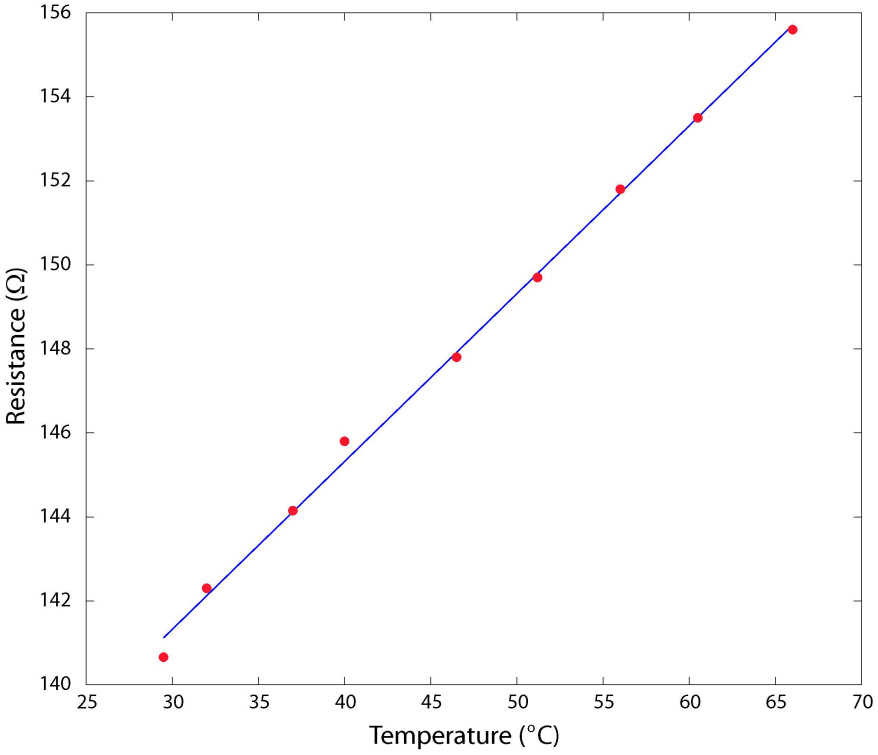

Fig. S7: Resistor calibration. Blue line shows characteristic fit (with R2 = 0.9819) to measured temperature dependence (red circles) of on-chip resistors. Such fitted functions are used to determine temperature from resistance during temperature and voltage sweep experiments.

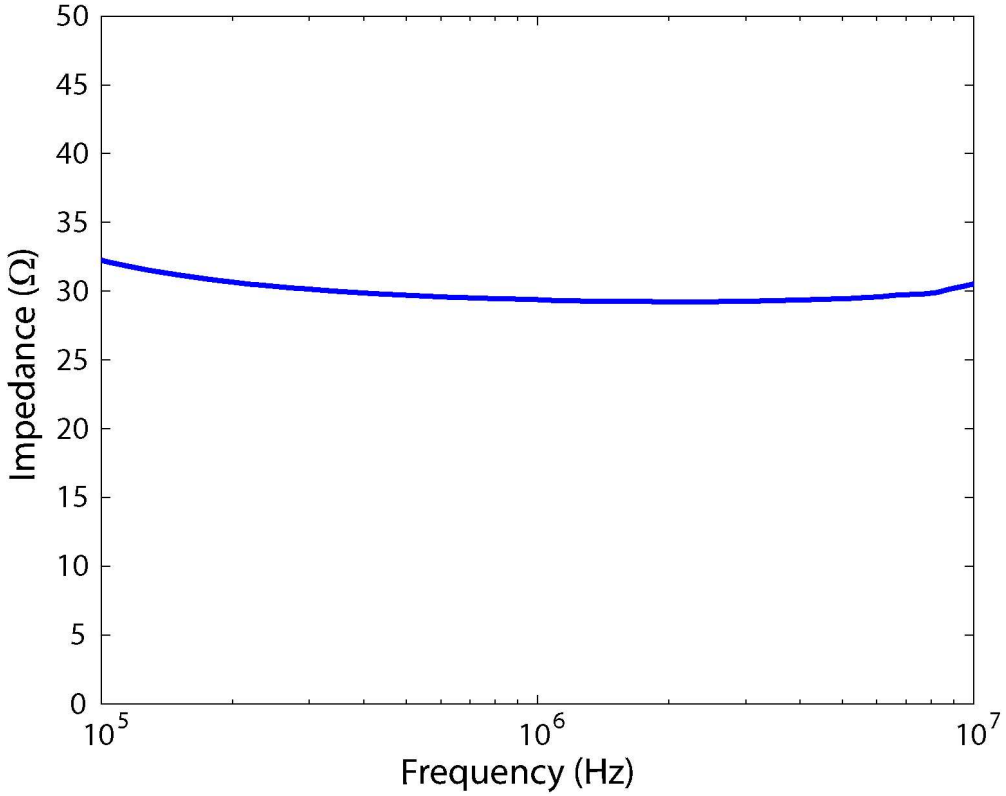

Fig. S8: Impedance measurements. Magnitude of impedance of a single well on the 16-well device loaded with culture media (oscillator voltage, 500 mV). Impedance is seen to be nearly constant (with 6.8% deviation) across two orders of magnitude in frequency.

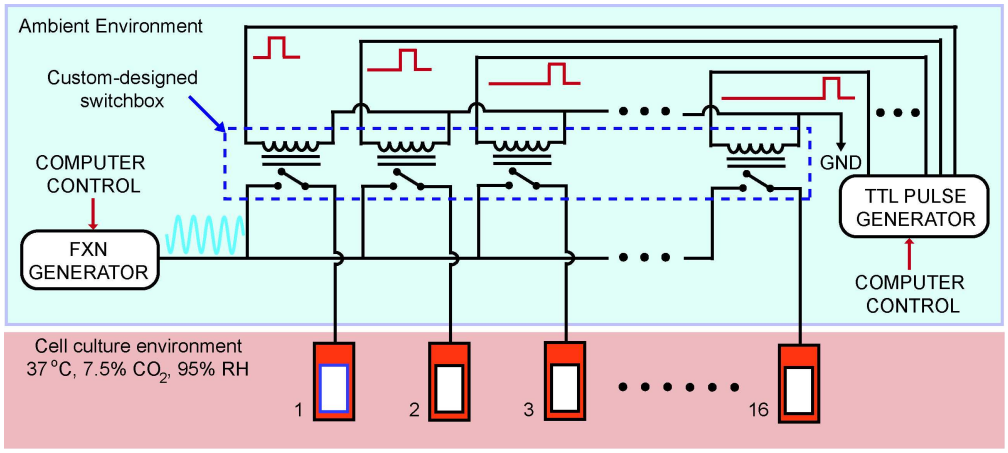

Fig. S9: Electrical stimulation setup. A custom-designed computer-controlled relay box (dashed line) switches sinusoidal waveforms from a function generator to each individual electrode site. The entire electrical stimulation system resides outside of the incubator while the electrode array resides within the incubator at physiological conditions. Resistance measurements from each temperature sensitive-resistor at each electrode site are logged via a USB-controlled resistance logging unit. Steady-state temperatures are determined by fitting logged values to pre-determined calibration curves.

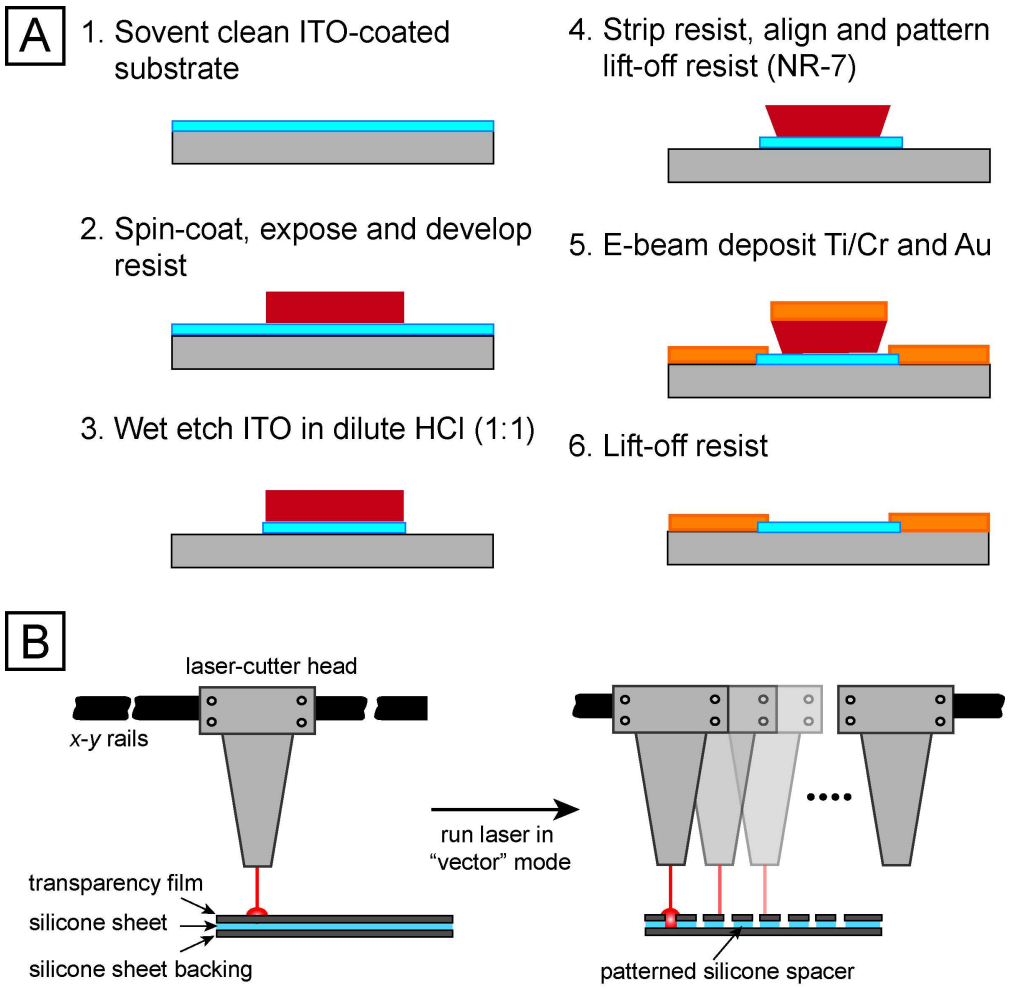

Figure S10: Fabrication processes. (A) Dual mask process for patterning electrode sites, temperature sensing resistors and routing. (B) Maskless process for fabricating silicone spacers to define volume for each electrode well.

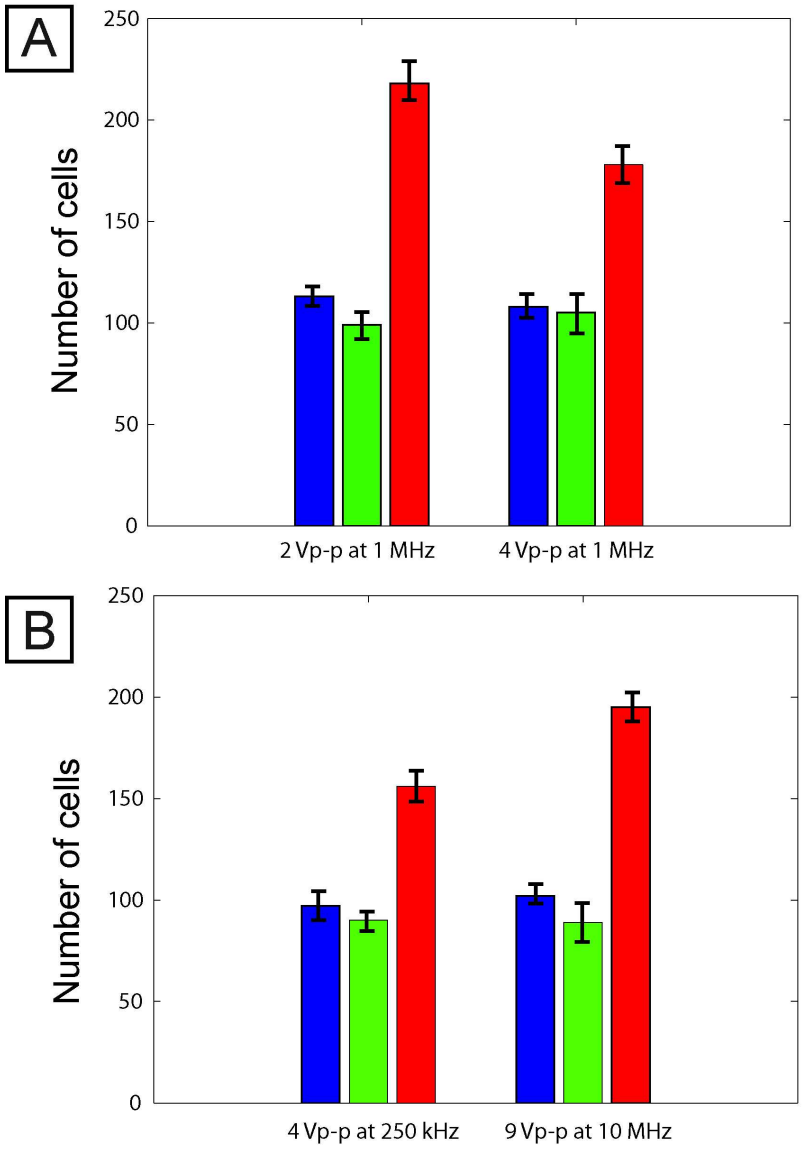

Figure S11: Proliferation assays. Cell counts from two conditions of the voltage sweep at 2 Vp-p at 1 MHz and 6 Vp-p at 1 MHz (A) and two conditions of the frequency sweep at 4 Vp-p at 250 kHz and 9Vp-p at 10 MHz. Bars represent average cell counts after seeding and before exposure to electric-field stimulus (blue), 16 hours after exposure to stimulus (green) and 32 hours after exposure (red). Error bars represent one standard deviation.